TITLE PAGE

Title: βARKct gene-therapy improves β_2-adrenergic receptor-dependent neoangiogenesis following hindlimb ischemia.

Authors: Alessandro Cannavo, Daniela Liccardo, Anastasios Lymperopoulos, Giuseppina Gambino, Maria Loreta D'Amico, Franco Rengo, Walter J Koch, Dario Leosco, Nicola Ferrara, Giuseppe Rengo

Authors affiliations: *Division of Geriatrics, Department of Translational Medical Sciences, Federico II University of Naples, Italy (A.C.; D.Li.; G.G.; M.L.D.A.; D.Le.; N.F.; G.R.); Center for Translational Medicine, Temple University, Philadelphia, PA (A.C.; D.Li.; W.J.K.); Department of Pharmaceutical Sciences, Nova Southeastern University College of Pharmacy, Fort Lauderdale, FL, USA (A.L.); Salvatore Maugeri Foundation, IRCCS, Scientific Institute of Telese Terme (BN) (F.R.; G.R.)* .

RUNNING TITLE PAGE

Running title: βARKct improves angiogenesis in ischemic hindlimb

Corresponding Author:

Prof. Dario Leosco

Department of Translational Medical Sciences

Federico II University

Via Pansini 5

80131, Naples

Italy

Tel: +39 0817463677

Fax: +39 0817463677

Email: dleosco@unina.it

Document Statistics:

32 text pages;

9 Figures;

43 References;

Abstract 250 words;

Introduction 444 words;

Results 1614;

Discussion 1237

Non-standard abbreviations: HI- Hindlimb Ischemia; βAR- β adrenergic receptor; βARKct- β adrenergic receptor kinase C-terminal peptide; GRK2- G protein coupled receptor kinase 2; GFP- Green Fluorescent Protein; Ad- Adenovirus; eNOS- endothelial nitric oxide synthase; NO-nitric oxide; BrdU-Bromodeoxyuridine (5-bromo-2'-deoxyuridine); BAEC- Bovine Aortic Endothelial Cell; EC- Endothelial Cell

ABSTRACT

Following hindlimb ischemia (HI) increased catecholamine levels within the ischemic muscle can cause dysregulation of β_2-adrenergic receptor (β_2AR) signaling leading to reduced revascularization. Indeed, in vivo β_2AR overexpression, via gene therapy, enhances angiogenesis in a rat model of HI. G protein-coupled receptor kinase 2 (GRK2) is a key regulator of βAR signaling, and βARKct, a peptide inhibitor of GRK2, has been shown to prevent βAR down-regulation and to protect cardiac myocytes and stem cells from ischemic injury, through restoration of β_2AR protective signaling (i.e. Akt/eNOS). Herein, we tested potential therapeutic effects of adenoviral-mediated βARKct gene transfer in an experimental model of HI and its effects on βAR signaling and on endothelial cell (EC) function *in vitro*. Accordingly, in this study, we surgically induced HI in rats by femoral artery resection (FAR). Fifteen days of ischemia resulted in significant βAR down-regulation that was paralleled by an about 2-fold increase in GRK2 levels in the ischemic muscle. Importantly, *in vivo* gene transfer of the βARKct in the hindlimb of rats at the time of FAR resulted in a marked improvement of hindlimb perfusion, with increased capillary and βAR density in the ischemic muscle, compared to control groups. The effect of βARKct expression was also assessed, *in vitro* in cultured ECs. Interestingly, in ECs expressing the βARKct, fenoterol, a β_2AR-agonist, induced enhanced β_2AR pro-angiogenic signaling and increased EC function. In conclusion, our results suggest that βARKct gene-therapy and subsequent GRK2 inhibition promotes angiogenesis in a model of HI by preventing ischemia-induced β_2AR downregulation.

INTRODUCTION

Peripheral arterial occlusive disease and its most advanced form, critical limb ischemia, represent a major clinical problem affecting 10-15% of the aged adult population (Norgren et al., 2007). Despite advances in endovascular revascularization and drug therapies, its prognosis remains poor with about 40% of patients requiring limb amputation. Therefore, new therapeutic options are urgently needed. In this regard, therapeutic angiogenesis has emerged as a promising investigational strategy for the treatment of patients with limb ischemia and gene therapy has been established as a potential method to manipulate levels/activity of key molecules in order to induce revascularization in patients with ischemic cardiovascular diseases (Rajagopalan et al., 2003; Kusumanto et al., 2006; Lederman et al., 2002; Nikol et al., 2008; Belch et al., 2011; Pugh and Ratcliffe, 2003). Angiogenesis is a biological process that generates new blood vessels from existing vasculature (Carmeliet 2005). In physiological conditions, this process occurs during embryonic development, pregnancy and through the ovarian cycle, but angiogenesis is also reactivated in a variety of pathologic conditions including ischemia, inflammation, wound healing, tumor growth, and diabetic retinopathy (Melillo et al., 1997; Rafii and Lyden, 2003). Importantly, in all these processes, angiogenesis is primarily regulated via endothelial cell (EC) proliferation and migration (D'Amore and Thompson, 1987). At the molecular level, it is known that the β_2-adrenergic receptor (β_2AR), the most abundant βAR isoform in ECs, is involved in the control of these functions (Howell et al., 1988). However, ischemia can result in increased sympathetic catecholamine levels that can cause β_2AR signaling dysfunction in ECs, resulting in an inadequate angiogenic response and loss of tissue integrity and/or function (Iaccarino et al., 2005; Rengo et al., 2012).

Mechanistically, G protein-coupled receptor kinases (GRKs) phosphorylate and desensitize activated βARs, thus preventing deleterious receptor overstimulation, but chronically this process continues through receptor internalization and degradation (Rengo et al., 2011). GRK2 is the isoform that appears most important for regulated βARs in muscle (Rengo et al., 2011). The βARKct, a peptide derived from the carboxyl terminal portion of GRK2 that blocks Gβγ recruitment of this kinase to the

activated membrane-embedded receptor, can inhibit βAR desensitization and improve signaling down-regulation/desensitization (Cannavo et al., 2013a; Rengo et al., 2009b; Salazar et al., 2013). Of note, different reports have proposed βARKct as a new therapeutic molecule for various model of cardiovascular disease, mainly through the potentiation of β_2AR signaling (Cannavo et al., 2013a; Khan et al., 2014; Salazar et al., 2013). Accordingly, since the effects of βARKct and GRK2 manipulation on EC function and angiogenesis is not well understood, we posited that this peptide could have the potential to improve post-ischemic re-vascularization through restoration of β_2AR signaling/function both *in vivo* and *in vitro*.

METHODS

Rat hindlimb ischemia model and in vivo gene therapy.

Hindlimb ischemia was induced in adult Sprague-Dawley male rats (300 grams) by excision of the right common femoral artery, as previously reported (Leosco et al. 2007). Briefly, rats were anesthetized with isoflurane (2%, v/v). A surgical incision was made in the skin overlying the middle portion of the right hind limb. After ligation of the proximal end of the femoral artery, the distal portion of the saphenous artery was legated, and the artery and all side branches were dissected free and excised. Then the skin was closed with a 2.0 silk suture. Sham-operated animals underwent the same procedure without ligation and excision of the right common femoral artery. In a group of rats receiving in vivo gene therapy, a silastic catheter was placed into the femoral artery distal to the resection, through which a solution containing 10^{12} total viral particles of an adenovirus (Ad) encoding for βARKct or GFP, or vehicle (saline), was infused into the hindlimb and allowed to remain there for 30 minutes while the saphenous vein was temporarily occluded. Afterwards, the virus was removed through the catheter, the common femoral artery removed and the wound closed in layers. All animal care and experimental protocols were approved by the Ethics Committee for the Use of Animals in Research of our Institution.

β-Adrenergic Receptor Radioligand Binding

Plasma Membrane fractions from excised skeletal muscles (gastrocnemius) were prepared and used for βAR radioligand binding studies using the non-selective βAR antagonist ligand (^{125}I)-Cyanopindolol (^{125}I-CYP), as described previously (**Rengo et al. 2010**). The concentration of 125I-CYP used in each series of reactions (assay) was 68.9 pmol/ml CYP and total activity was 5 μCi (125I-CYP specific activity: 2.2 Ci/μmol).

Cell Culture

Bovine aortic endothelial cells (BAECs) were purchased from Lonza and maintained in Dulbecco's modified Eagle's medium (DMEM) supplemented with 10% FBS, 200 mg/ml L-glutamine, 100 units/ml penicillin, and 100 μg/ml streptomycin at 37°C in 95% air and 5% CO2. For all experiments, BAECs were used at passage 14 or less. Primary ECs were isolated from Wild-type (WT) and global eNOS knockout (KO) mice. Thoracic aorta was dissected, placed rapidly in ice-cold PBS and gently flushed using 1-mL syringe fitted with 23-G needle to remove blood clots. After removing the fibro-adipose tissue and small lateral blood vessels, the aorta was cut into 1-mm rings. The aortic rings were further washed using sterile ice-cold PBS and then transferred in six-wells plate coated with Matrigel (Corning, USA). The aortic rings were then covered with few drops of matrigel and Endothelial cell growth medium (DMEM with 25 mM HEPES,10% FBS, 90 μg/mL heparin sulfate, 90 μg/mL endothelial cell growth factor, 10,000 U/mL penicillin, 10 mg/mL streptomycin). The ECs sprouts were observed after two days. On the fourth-day the aortic rings were carefully removed and the ECs were allowed to proliferate in Matrigel until reaching confluence. To collect the ECs, matrigel were digested using dispase then cells were cultured to 80% confluence and then sorted for CD-31 using CD-31 Endothelial Cell Dynabeads® (life technology, USA) according to the manufacturer's instructions. The CD31+ cells were then plated and used for experimental procedures.

BAECs and primary ECs were stimulated with fenoterol (Sigma Aldrich, USA; 1 μM) for 5, 15 and 30 minutes and for 6 hours for immunoblot assay. While 6 and 24 hours of fenoterol stimulation were used to assess the EC function. Prior to fenoterol stimulation some cells was pre-treated for 30 minutes with the highly selective β_2AR-antagonist ICI 118551 (IC50 Value**:** 1.2 nM (Ki); 10 μM), as previously reported (Cannavo et al. 2013c).

Adenoviral constructs

For *in vivo* and *in vitro* procedure we used recombinant adenoviral (Ad) vectors encoding for the bovine wild-type GRK2 gene (Ad-GRK2) or one encoding for the C-terminal region containing the last 194

amino acids of GRK2, which makes up the βARKct (Ad-βARKct). An Ad encoding for the Green fluorescent protein (Ad-GFP) was used as control (Lymperopoulos et al., 2008).

***In vitro* Adenoviral infection**

Infections were accomplished on ECs at 50–60% confluence. Cells were infected with adenovirus expressing GRK2, βARKct or GFP as control at a MOI of 100 per cell for 24 hours at 37°C, as previously described (Lymperopoulos et al., 2008; Homan et al., 2014). The cells were then incubated in fresh medium for an additional 24 h prior to experimentation.

Immunoblot

Cells and skeletal muscle samples were lysed in a RIPA buffer with protease and phosphatase inhibitors cocktail (Roche, CH) as previously described (Cannavo et al., 2013b). Protein concentrations in all lysates were measured using a dye-binding protein assay kit (Bio-Rad, USA) and a spectrophotometer reader (Biorad, USA) at a wavelength of 750 nm. Protein levels of GRK2 (Santa Cruz Biotechnology, Inc.,USA 1:1.000), pAkt (Sigma-Aldrich, USA 1:1000), tAkt (Santa Cruz Biotechnology, Inc, USA 1:1.000), eNOS (Cell Signaling, 1:1000), p-eNOS (Cell Signaling, 1:1000), β_2AR (Santa Cruz Biotechnology, Inc, USA 1:1000), p-β_2AR (EMD Millipore Corporation, Billerica, MA, USA 1:1000) and GAPDH (EMD Millipore Corporation, Billerica, MA, USA 1:1000) were assessed. Secondary antibodies were purchased from Amersham Life Sciences Inc. Bands were visualized by enhanced chemiluminescence (ECL; EMD Millipore Corporation, Billerica, MA, USA) according to the manufacturer's instructions, and were quantified using densitometry (Chemidoc, Biorad, USA). Each experiment and densitometric analysis was separately repeated three times.

Immunohistochemistry

Immunohistochemistry was performed as previously described (Cannavo et al. 2013b). Briefly, deparaffinized slides were treated with the following polyclonal antibodies: GRK2 (Santa Cruz, 1:200), GFP (Santa Cruz, 1:200). The visualization was performed using an ABC kit (Thermo Scientific, Rockford,IL, USA) and diaminobenzidine (DAB; Pierce) chromogen.

Confocal microscopy

Confocal microscopy studies were performed as previously described (Cannavo et al., 2013c). Following fixation with 3% paraformaldehyde, cells were incubated with an anti-β_2AR antibody (1:200 anti-rabbit IgG, Santa Cruz) in 1% BSA. Next, the cells were incubated with the secondary rabbit polyclonal antibodiy (1:200, Texas Red coniugated; Sigma). Visualization with confocal laser scanning microscopy was performed at 568 nm (Cy3) with a Zeiss 510 confocal laser scanning microscope. The fluorescent data sets were analyzed by LSM 510 software.

EC function *in vitro* assays

For EC proliferation and migration assays, the stimulation was performed in presence of DMEM supplemented with 2% FBS. Cell migration was assessed by wound-healing scratch assay performed in 12-well tissue culture plates. Twenty-four hours after Ad infection, scratches were made using 100 µL pipette tips and the wells were washed twice with PBS. Following 6 hours of Fenoterol (1 µM) stimulation the cells were fixed in 3.7% paraformaldehyde and stained with 0.1% crystal violet staining solution as previously described (Liu et al. 2013). Photographs were taken on Nikon TE2000-U inverted microscope connected to a Nikon camera. Quantification of cell migration was done by measuring the distance between 10 random points within the wound edge. Gap distance of the wound was measured using ImageJ software, and the data were normalized to the average of the wound of control cells fixed at the time of scratches.

Proliferation was assessed by quantitative measurement of DNA synthesis using a 5-bromo-2'-deoxyuridine (BrdU) ELISA kit (Roche, CH), accordingly to manufacturer instructions. Briefly, after 24 hours from Ad infection, BrdU was added to the medium at a final concentration of 10 μM, and the cells were incubated for 6 or 24 hours in presence or absence of fenoterol (1 μM). BrdU incorporation was then assayed using a colorimetric detection system. The number of proliferating cells was represented by the level of BrdU incorporation, which directly correlates to the color intensity and the absorbance values.

Nitric oxide (NO) measurement

BAECs or murine aortic endothelial cells, infected with Ad-βARKct and –GFP, were stimulated or not with fenoterol (1 μM) for 6 hours. Following stimulation, the concentrations of nitric oxide (NO) in the culture medium were measured using the NO colorimetric assay kit (BioVision, Mountain View, CA) according to the manufacturer's protocol. Briefly, the nitrate was converted to nitrite utilizing nitrate reductase, then the nitrite was converted to a deep purple azo compound using Griess reagent. The amount of the azochromophore was detected by the colorimetric determination at 540 nm using a microplate reader.

Blood flow determination

Blood flow (BF) in the posterior tibial artery of ischemic and non-ischemic hindlimb was evaluated by ultrasound (US) Doppler (using a Visual SONICS VeVo 770 imaging system with a 708 MHz scanhead) in isofluorane-anaesthetized rats (2% v/v) immediately before and at 12 hours, 3, 7, 10 and 15 days after surgery, as previously described (Ciccarelli et al., 2011). Data are expressed as ischemic to non-ischemic ratio. Fifteen days after surgery, blood flow was also measured by dyed beads assay, as previously described (Ciccarelli et al., 2011).

Histology

Tibialis anterior muscle specimens were fixed in 4% paraformaldehyde and embedded in paraffin. After deparaffinization and rehydration, 5-μm-thick sections were prepared, mounted on glass slides. Capillary density was performed as previously described (Ciccarelli et al., 2011; Rengo et al., 2013).

Statistical analysis

Data are summarized as mean±SEM. Comparisons were made with the use of t-tests or ANOVA, as appropriate. A Bonferroni correction was applied to the probability values whenever multiple comparisons arose. Values of $p<0.05$ were considered significant.

RESULTS

βARKct gene-therapy improves angiogenesis and restores βAR density in the ischemic hindlimb.

Following hindlimb ischemia (HI), increased levels of catecholamines (CAs) are responsible for βAR-signaling dysfunction, leading to reduced angiogenesis in the ischemic tissue (Sorriento et al., 2012; Iaccarino et al., 2005). Importantly, a similar mechanism has been observed also in the heart, where βARKct gene-therapy has been proposed as a potential strategy to prevent βAR dysregulation and to ameliorate cardiac response to ischemia (White et al., 2000). However, the effects of βARKct gene-therapy in a model of HI have not been specifically investigated. Thus, we surgically induced HI in adult male Sprague-Dawley rats by resection of the right common femoral artery (FAR). A group of sham-operated rats served as control. At 15 days post-surgery, blood flow was measured by a dyed beads perfusion assay showing a significant reduction in hindlimb perfusion in the ischemic muscle of the group undergoing FAR compared to sham-operated rats, as expected (**Figure 1A**). In line with previous reports (Iaccarino et al., 2005), 2 weeks after surgically induced ischemia, we observed a significant reduction in βAR density within the ischemic skeletal muscle compared to the skeletal muscle of sham-operated rats (**Figure 1B**). The reduction in βAR plasma membrane density was paralleled by a robust up-regulation of GRK2 protein levels in the ischemic skeletal muscle compared with the limbs of sham-operated rats (**Figure 1C**). Next, to test the effects of βARKct expression, a group of rats was injected into the femoral artery with an Adenovirus (Ad) encoding for βARKct (Ad-βARKct) or Ad-GFP, as control, at the time of FAR. A separate group of animals were treated with a saline injection, to provide an additional control to assess any potential effect of Ad infection or GFP expression (**Figure 2A**). At the end of the study period, transgene expression was successfully detected by immunohistochemistry and resulted in predominant perivascular localization (**Figure 2B**). However, consistent with previous reports (**Iaccarino et al. 2005**), transgene expression was not limited to the endothelium, but was also observed in the skeletal muscle. Moreover, we assessed βARKct expression in the ischemic skeletal muscle of rats at the end of the study

period by immunoblotting (**Figure 2C)**. As expected, βARKct was clearly detectable in the muscle of rats treated with Ad-βARKct (**Figure 2D)**.

Next, to evaluate the effects of βARKct gene-therapy on post-ischemic angiogenesis, blood flow was measured in all groups by Doppler over the course of 15-day study period. As shown in **figure 3A**, immediately after FAR, blood flow was not detectable in the ischemic tibial posterior artery of all study groups. As expected, blood flow was partially and progressively restored in rats treated with saline or GFP over the 15-day study period (**Figure 3A**). However, βARKct gene therapy resulted in a significant increase in blood flow compared to control groups (**Figure 3A**). Data from the dyed beads perfusion assay confirmed these results (**Figure 3B**). In line with blood flow and perfusion data, histological analysis of the tibial anterior muscle revealed that 15 days of hindlimb ischemia induced a robust capillary rarefaction in saline- and Ad-GFP-treated rats (**Figure 3C**). Of note, we found a complete restoration of the capillary density in βARKct treated ratsthat was not statistically different to that measured in sham-operated animals (**Figure 3C**).

Finally, we assessed βAR plasma membrane density in the ischemic gastrocnemius from all study groups (**Figure 3D**). In line with previous reports (Iaccarino et al., 2005), a significant down-regulation of total βAR density was observed in saline- and GFP-treated groups compared to sham-operated animals. More importantly, βARKct gene-therapy resulted in the restoration of βAR density in the ischemic muscles, at levels that were almost similar to sham groups.

βARKct improves *in vitro* β_2AR-signaling in Endothelial cells (ECs).

Our *in vivo* data showing that βARKct-dependent re-vascularization is associated with a restoration of βAR density in the ischemic skeletal muscle prompted us to investigate the effects of this peptide on EC function. Bovine aortic ECs (BAECs) were stimulated *in vitro* with the selective β_2AR-agonist fenoterol (1 μM) (January et al., 1997) to test activation of Akt and endothelial NO synthase (eNOS), since these protein are known to be nodal regulators of EC function (Howell et al., 1988).

Indeed, we found that fenoterol was able to increase both Akt and eNOS activation following 15 minutes of stimulation (**Figure 4A-B**). Notably, pre-treatment of cells for 30 minutes with the selective β_2AR antagonist ICI-118,551 (10 μM) completely prevented the ability of fenoterol to increase in Akt and eNOS phosphorylation (**Figure 4A-B**), indicating that these effects are completely dependent on β_2AR activation. Next, ECs were infected *in vitro* with Ad-GRK2 or Ad-βARKct or Ad-GFP (as control) and, we assessed the effects of fenoterol on β_2AR phosphorylation/desensitization (p-β_2AR), by measuring phospho-threonine (pThr) 384 levels of the bovine β_2AR (i.e. the homologous residue to the threonine targeted by GRK2 in the human β_2AR, triggering rapid receptor desensitization) (Fredericks et al., 1996). In absence of agonist stimulation, there were no differences in terms of β_2AR phosphorylation between GFP, GRK2 and βARKct infected cells (**Figure 5A**). Five minutes of fenoterol stimulation resulted in a significant increase in p-β_2AR levels in all EC groups compared to unstimulated ECs. However, GRK2 overexpression induced a further significant increase in p-β_2AR levels compared to both GFP and βARKct cells, suggesting that increased GRK2 activity is responsible for augmented β_2AR phosphorylation and consequent desensitization also in ECs (**Figure 5A**). Next, we tested the direct effects of GRK2 and βARKct on fenoterol-dependent Akt and eNOS activation (**Queen et al., 2006; Figueroa et al., 2009**). Indeed, in GFP- and in βARKct-treated cells, 15 minutes of fenoterol administration induced a significant enhancement in both Akt and eNOS phosphorylation (**Figure 5B-C**), while GRK2 overexpression resulted in a blunted activation of these factors. Notably, following 15 minutes of fenoterol stimulation no significant changes in GRK2 protein levels were observed between GFP- and in βARKct-infected cells (**Figure 5D**).

Next, we tested the impact of longer fenoterol stimulation on β_2AR signaling in ECs. Interestingly, following 6 hours of fenoterol administration, GRK2 expression was increased in both GFP and βARKct cells, at levels almost comparable, but statistically different, to those observed in Ad-GRK2 treated cells (**Figure 6A**). However, a robust β_2AR phosphorylation/desensitization was evident only in GFP and GRK2 cells. Further, p-β_2AR levels were significantly reduced in presence of βARKct (**Figure**

6B). Consistent with increased β_2AR desensitization, long-term fenoterol stimulation resulted in decreased Akt (**Figure 6C**) and eNOS (**Figure 6D**) activation in both GFP and GRK2 overexpressing cells. In contrast, the presence of βARKct, which prevented β_2AR phosphorylation and subsequent desensitization (**Figure 6B**), resulted in an increased activation of Akt and eNOS, at levels comparable to basal unstimulated conditions (**Figure 6C-D**). These results strongly suggest a potential role of βARKct in preventing GRK2-dependent β_2AR phosphorylation and consequent receptor down-regulation. In order to confirm this hypothesis, we performed plasma membrane purifications in extracts obtained from BAECs infected with GFP and βARKct, and either left un-stimulated or stimulated with both with fenoterol for 6 hours, and we found a significant reduction in β_2AR plasma membranes levels in GFP cells (**Figure 7A-B**). Further, internalized β_2AR levels were increased compared to unstimulated cells. In contrast, βARKct expression prevented the effects of fenoterol on β_2AR-plasma membrane downregulation (**Figure 7A-B**). In line with these results, confocal microscopy experiments, confirmed that β_2AR was mainly localized at cytosolic level following fenoterol stimulation in GFP ECs (**Figure 7C**). In contrast, βARKct expression resulted in predominant β_2AR localization at the plasma membrane similar to that observed in unstimulated cells (**Figure 7C**).

βARKct enhances *in vitro* EC function in response to selective β_2AR stimulation

Since, our data above showed that βARKct prevented the fenoterol induced β_2AR desensitization/downregulation and rescued associated pro-angiogenic signaling, we evaluated the effects of β_2AR-agonism on EC function. We first assessed NO release, since it has been demonstrated to be a potential modulator of EC function. As showed in **Figure 8A**, following 6 hours of fenoterol stimulation, we observed a significant increase in NO release in GFP cells, compared to unstimulated ones. Of note, following fenoterol stimulation in the presence of βARKct, we observed a more pronounced NO release compared to all cell groups.

Next, we assessed the effects of β_2AR-agonism on EC function. We evaluated EC migration performing a wound healing scratch assay under basal condition and after challenge with β_2AR agonist. As shown in **Figure 8B**, under basal conditions, the expression of βARKct did not induce any significant effect on cell migration compared to GFP cells. Importantly, fenoterol stimulation resulted in a ≈2-fold increase in migration in GFP cells and, the presence of βARKct, induced significantly enhanced EC migration in response to β_2AR stimulation that was almost double to that observed in control GFP cells. Similar results were obtained in an EC proliferation assessed by 5-bromo-2'-deoxyuridine (BrdU) incorporation (**Figure 8C)**. Fenoterol induced a significant increase in EC proliferation in GFP cells compared to non-stimulated cells at both 6 and 24 hours, and βARKct expression induced a robust proliferative response to β_2AR-agonism that was significantly higher than that observed in GFP treated cells at both time points (**Figure 8C**).

Finally, in order to study the role of βARKct on β_2AR-dependent eNOS activation, we isolated primary ECs from the aorta of wild-type (WT) and eNOS knockout (KO) mice. The ECs were then infected with Ad-GFP and Ad-βARKct. Importantly, the lack of eNOS almost completely prevented the effects of βARKct on fenoterol-dependent increase in EC migration (**Figure 9A**) and proliferation (**Figure 9B**) compared to WT cells. In line with these results, at molecular level, we observed that the lack of eNOS abolished the ability of βARKct to activate/rescue β_2AR-dependent Akt activation (**Supplemental Figure 1A-B**) and to increase NO release following fenoterol stimulation **(Figure 9C**).

DISCUSSION

There is extensive literature supporting the therapeutic value of βARKct gene therapy to ameliorate cardiac function and remodeling following MI (Cannavo et al. 2013a), especially for its ability to block GRK2-dependent β_2AR dysfunctional signaling (Cannavo et al. 2013a, Khan et al., 2014; Salazar et al., 2013). Herein, we report for the first time the effects of βARKct gene therapy in a rat model of hindlimb ischemia (HI). In particular, we show that βARKct is a new potential therapeutic tool to improve post-ischemic angiogenesis through preservation of β_2AR signaling in the endothelium. We observed that ischemia induces the up-regulation of GRK2 protein levels in skeletal muscle and this event appears to be critical in the processes of re-vascularization of the ischemic hindlimb, since it is associated with βAR-desensitization/downregulation. Importantly, the present study confirms the relevant role of endothelial β_2AR in the control of re-vascularization *in vivo* and EC function *in vitro*. In this context, previous studies have reported a crucial role of β_2AR at promoting *in vivo* post-ischemic revascularization and, in particular, its functional relevance in the regulation of EC function *in vitro* has emerged as a key mechanism (Iaccarino et al., 2005). β_2AR KO mice exhibited impaired re-vascularization following ischemia with a high rate of tissue necrosis and subsequent auto-amputation of ischemic limbs (Iaccarino et al., 2005). Moreover, in a rat model of HI, when β_2AR is downregulated, gene therapy using the receptor resulted in improved revascularization of the ischemic limb (Iaccarino et al., 2005).

Importantly, no mechanism has been proposed for triggering ischemic-mediated β_2AR dysfunction. Accordingly, the ability of GRK2 to regulate βAR signaling and function in the heart has been well established (Cannavo et al., 2013a; Huang et al., 2011) and therapies that inhibit the activity of this kinase on receptor phosphorylation/downregulation at the plasma membrane have been shown to be strongly protective towards cardiac injury and stress in part, by restoring myocardial βAR signaling abnormalities (Cannavo et al., 2013a; Rengo et al., 2009a; Rengo et al., 2011). Herein, we show that the resection of the common femoral artery in rats, a well recognized model of peripheral artery disease (Leosco et al., 2007; Iaccarino et al., 2005), results in ≈2-fold increase in GRK2 levels in the ischemic

gastrocnemius compared to sham-operated rats. Moreover, we confirmed that GRK2 up-regulation is paralleled by significant βAR downregulation in the ischemic skeletal muscle. Thus, we tested the *in vivo* properties of Ad-mediated intra-arterial gene transfer of the GRK2 inhibitor βARKct on HI. Importantly, our data show that βARKct expression in the ischemic tissue induces a significant increase in blood flow recovery and perfusion of the ischemic hindlimb compared to control groups (Saline- and GFP-treated) at 15 days post-FAR. Of note, this result is associated with a significant increase in capillary density suggesting improved post-ischemic angiogenesis. As reported by others (Iaccarino et al., 2005), ischemia is associated with significant βAR downregulation and dysfunction in the affected muscle. Consistently, in our control groups undergoing HI, βAR density is reduced in the ischemic muscle. However, 15 days of βARKct expression significantly improved βAR density in the ischemic hindlimb, almost to levels observed in sham-operated rats, thus suggesting a possible explanation for the beneficial effects of this therapeutic strategy on *in vivo* revascularization.

Since a pivotal role of β_2ARs exists for EC function (Iaccarino et al., 2005; Ciccarelli et al., 2011; Howell et al., 1988), particularly in respect to the regulation of postnatal ischemic angiogenesis, our mechanistic focus targeting GRK2 activity was to investigate the impact of βARKct on EC function *in vitro*. In BAECs, we have observed that GRK2 overexpression, obtained via Ad-mediated gene transfer, significantly impairs both cell migration and proliferation in response to selective β_2AR stimulation. This shows that indeed GRK2 has influence at the level of the β_2AR and can be a mediator of dysregulation of the system. At the molecular level, these deleterious effects exerted by GRK2 on EC function are paralleled by β_2AR dysfunctional signaling, as suggested by levels of receptor phosphorylation and reduced Akt and eNOS activation following acute fenoterol stimulation (5-15 minutes, respectively). Interestingly, following 6 hours of fenoterol stimulation, these negative effects are also observed in GFP infected cells, but it is important to underline that at this time-point fenoterol induces a strong up-regulation of endogenous GRK2 levels (Figure 6). However, after 15 minutes of fenoterol stimulation, a time-point where GRK2 is not up-regulated, Ad-GFP treated ECs show reduced levels of p-β_2AR and,

increased level of Akt and eNOS activation when compared to Ad-GRK2 treated cells, thus indicating higher responsiveness to β_2AR activation (Figure 5). Of further importance, βARKct expression improves EC migration and proliferation and preserves β_2AR signaling and function, after fenoterol stimulation (Figure 7). These data suggest that βARKct is able to enhance β_2AR signaling and to improve EC function following fenoterol administration.

Study limitations. GRK2 has been shown to directly interact with and inhibit both Akt and eNOS (Brinks at al., 2010; Huang at al., 2013) therefore, it is quite likely that, some of the observed effects of βARKct are due to direct inhibition of GRK2 acting on Akt/eNOS and independently of the β_2AR. However, our results strongly suggest that acute β2AR stimulation by fenoterol can directly activate Akt and eNOS in ECs in vitro and that, while βARKct expression does not affect the acute action of fenoterol, it ameliorates later effects of fenoterol on β2AR phosphorylation, enhancing NO release in these cells. Moreover, our data obtained in eNOS KO ECs support the hypothesis that the preservation of β_2AR/eNOS axis is relevant for the positive effects of βARKct in ECs. It is important to underline that we cannot exclude any potential involvement of other cell types (i.e. skeletal muscle cells or smooth muscle cells) other than ECs and endothelial progenitor cells (EPCs) for which recently has been proposed a relevant role in post-ischemic angiogenesis *in vivo* (Galasso et al., 2013). In this regard, it has been recently demonstrated that in C2C12 myoblasts, GRK2 overexpression lead to a significant impairment in cell differentiation, thus suggesting for this kinase a relevant role in skeletal muscle myogenesis (Garcia-Guerra et al 2014). Thus, we cannot exclude additional effects of βARKct in skeletal muscle cells in our *in vivo* model. As an addition limitation, as reported by other previously (Iaccarino et al., 2005) and as shown in our immunohistochemistry (Supplemental Figure 1), the gene delivery technique we used results in a predominant localization of the transgenes to the existing vascular structures within the ischemic tissue. Finally, in our *in vivo* study we measured total βAR density in the ischemic muscle of rats rather than β_2AR density. However, the β_2AR is known to be the main isoform expressed in EC and in the skeletal muscles (Osswald and Guimarães,1983; Guimarães and Moura, 2001; Lynch and Ryall,

2008), thus we can assume that part of the effects of HI and βARKct gene therapy on total βAR density might be ascribed to changes in β_2AR density. Moreover, our *in vitro* data in ECs have specifically investigated the effects of βARKct on β_2AR signaling and function, clearly demonstrating a protective effect of βARKct on β_2AR downregulation.

In conclusion, in the present study we provide novel evidence that βARKct expression and subsequent GRK2 inhibition positively regulates β_2AR signaling and function in ECs with relevant implications on post-ischemic angiogenesis. For this reason we propose βARKct gene therapy as a new therapeutic approach to re-establish blood flow to the limbs affected by critical ischemia.

Authorship Contributions

Participated in research design: Alessandro Cannavo, Daniela Liccardo, Giuseppe Rengo, Walter J. Koch and Dario Leosco

Conducted experiments: Alessandro Cannavo, Daniela Liccardo, Anastasios Lymperopoulos, Giuseppina Gambino, Maria Loreta d'Amico and Giuseppe Rengo

Contributed new reagents or analytic tools: Alessandro Cannavo, Daniela Liccardo, Giuseppe Rengo, Walter J. Koch and Dario Leosco.

Performed data analysis: Daniela Liccardo, Alessandro Cannavo, Giuseppe Rengo.

Wrote or contributed to the writing of the manuscript: Alessandro Cannavo, Daniela Liccardo, Giuseppe Rengo, Franco Rengo, Walter J. Koch, Nicola Ferrara and Dario Leosco.

REFERENCES

Belch J, Hiatt WR, Baumgartner I, Driver IV, Nikol S, Norgren L, Van Belle E (2011) Effect of fibroblast growth factor NV1FGF on amputation and death: a randomised placebo-controlled trial of gene therapy in critical limb ischaemia. Lancet **377**:1929–1937.

Brinks H, Boucher M, Gao E, Chuprun JK, Pesant S, Raake PW, Huang ZM, Wang X, Qiu G, Gumpert A, Harris DM, Eckhart AD, Most P, Koch WJ. (2010) Level of G protein-coupled receptor kinase-2 determines myocardial ischemia/reperfusion injury via pro- and anti-apoptotic mechanisms. Circ Res **107**:1140-1149.

Cannavo A, Liccardo D, Koch WJ (2013a) Targeting cardiac β-adrenergic signaling via GRK2 inhibition for heart failure therapy. Front Physiol 4: 264.

Cannavo A, Rengo G, Liccardo D, Pironti G, Scimia MC, Scudiero L, De Lucia C, Ferrone M, Leosco D, Zambrano N, Koch WJ, Trimarco B, Esposito G (2013b) Prothymosin alpha protects cardiomyocytes against ischemia-induced apoptosis via preservation of Akt activation. Apoptosis **18**:1252-1261.

Cannavo A, Rengo G, Liccardo D, Pagano G, Zincarelli C, De Angelis MC, Puglia R, Di Pietro E, Rabinowitz JE, Barone MV, Cirillo P, Trimarco B, Palmer TM, Ferrara N, Koch WJ, Leosco D, Rapacciuolo A (2013c) β1-adrenergic receptor and sphingosine-1-phosphate receptor 1 (S1PR1) reciprocal downregulation influences cardiac hypertrophic response and progression to heart failure: protective role of S1PR1 cardiac gene therapy. Circulation **128**:1612-1622.

Carmeliet P (2005) Angiogenesis in life, disease and medicine. Nature **438**: 932-936.

Ciccarelli M, Sorriento D, Cipolletta E, Santulli G, Fusco A, Zhou RH, Eckhart AD, Peppel K, Koch WJ, Trimarco B, Iaccarino G (2011) Impaired neoangiogenesis in β_2-adrenoceptor gene-deficient mice:

restoration by intravascular human β_2-adrenoceptor gene transfer and role of NFκB and CREB transcription factors. Br J Pharmacol **162**: 712-721.

D'Amore PA, Thompson RW (1987) Mechanisms of angiogenesis. Annu Rev Physiol **49**: 453-464.

Figueroa XF, Poblete I, Fernández R, Pedemonte C, Cortés V, Huidobro-Toro JP (2009) NO production and eNOS phosphorylation induced by epinephrine through the activation of beta-adrenoceptors. Am J Physiol Heart Circ Physiol. **297**: H134-143.

Fredericks ZL, Pitcher JA, Lefkowitz RJ Identification of the G protein-coupled receptor kinase phosphorylation sites in the human beta2-adrenergic receptor. (1996) J Biol Chem **271**: 13796-13803.

Galasso G, De Rosa R, Ciccarelli M, Sorriento D, Del Giudice C, Strisciuglio T, De Biase C, Luciano R, Piccolo R, Pierri A, Di Gioia G, Prevete N, Trimarco B, Piscione F, Iaccarino G (2013) β2-Adrenergic receptor stimulation improves endothelial progenitor cell-mediated ischemic neoangiogenesis. Circ Res. **112**: 1026-1034.

Garcia-Guerra L, Vila-Bedmar R, Carrasco-Rando M, Cruces-Sande M, Martín M, Ruiz-Gómez A, Ruiz-Gómez M, Lorenzo M, Fernández-Veledo S, Mayor F Jr, Murga C, Nieto-Vázquez I. (2014) Skeletal muscle myogenesis is regulated by G protein-coupled receptor kinase 2. J Mol Cell Biol 6:299-311.

Guimarães S, Moura D (2001) Vascular adrenoceptors: an update. Pharmacol Rev **53**: 319-56.

Homan KT, Wu E, Cannavo A, Koch WJ, Tesmer JJ (2014) Identification and characterization of amlexanox as a G protein-coupled receptor kinase 5 inhibitor. Molecules **19**: 16937-16849.

Howell RE, Albelda SM, Daise ML, Levine EM (1988) Characterization of beta-adrenergic receptors in cultured human and bovine endothelial cells. J Appl Physiol **65**: 1251-1257.

Huang ZM, Gold JI, Koch WJ (2011) G protein-coupled receptor kinases in normal and failing myocardium. Front Biosci **16**:3047-3060.

Huang ZM, Gao E, Fonseca FV, Hayashi H, Shang X, Hoffman NE, Chuprun JK, Tian X, Tilley DG, Madesh M, Lefer DJ, Stamler JS, Koch WJ (2013) Convergence of G protein-coupled receptor and S-nitrosylation signaling determines the outcome to cardiac ischemic injury. Sci Signal **6**:ra95.

Iaccarino G, Ciccarelli M, Sorriento D, Galasso G, Campanile A, Santulli G, Cipolletta E, Cerullo V, Cimini V, Altobelli GG, Piscione F, Priante O, Pastore L, Chiariello M, Salvatore F, Koch WJ, Trimarco B (2005) Ischemic neoangiogenesis enhanced by beta2-adrenergic receptor overexpression: a novel role for the endothelial adrenergic system. Circ Res **97**: 1182-1189.

January B, Seibold A, Whaley B, Hipkin RW, Lin D, Schonbrunn A, Barber R, Clark RB (1997) beta2-adrenergic receptor desensitization, internalization, and phosphorylation in response to full and partial agonists. J Biol Chem **272**: 23871-23879.

Khan M, Mohsin S, Toko H, Alkatib M, Nguyen J, Truffa S, Gude N, Chuprun K, Tilley DG, Koch WJ, Sussman MA (2014) Cardiac progenitor cells engineered with βARKct have enhanced β-adrenergic tolerance. Mol Ther **22**: 178-185.

Kusumanto YH, van Weel V, Mulder NH, Smit AJ, van den Dungen JJ, Hooymans JM, Sluiter WJ, Tio RA, Quax PH, Gans RO, Dullaart RP, Hospers GA (2006) Treatment with intramuscular vascular endothelial growth factor gene compared with placebo for patients with diabetes mellitus and critical limb ischemia: a double-blind randomized trial. Hum Gene Ther **17**: 683–691.

Lederman RJ, Mendelsohn FO, Anderson RD, Saucedo JF, Tenaglia AN, Hermiller JB, Hillegass WB, Rocha-Singh K, Moon TE, Whitehouse MJ, Annex BH (2002) Therapeutic angiogenesis with recombinant fibroblast growth factor-2 for intermittent claudication (the TRAFFIC study): a randomised trial. Lancet **359**: 2053–2058.

Leosco D, Rengo G, Iaccarino G, Sanzari E, Golino L, De Lisa G, Zincarelli C, Fortunato F, Ciccarelli M, Cimini V, Altobelli GG, Piscione F, Galasso G, Trimarco B, Koch WJ, Rengo F (2007) Prior exercise improves age-dependent vascular endothelial growth factor downregulation and angiogenesis responses to hind-limb ischemia in old rats. J Gerontol A Biol Sci Med Sci **62**: 471-480.

Lymperopoulos A, Rengo G, Zincarelli C, Soltys S, Koch WJ (2008) Modulation of adrenal catecholamine secretion by in vivo gene transfer and manipulation of G protein-coupled receptor kinase-2 activity. Mol Ther **16**: 302-307.

Lynch GS1, Ryall JG (2008) Role of beta-adrenoceptor signaling in skeletal muscle: implications for muscle wasting and disease. Physiol Rev **88**: 729-767.

Liu Y, Cao W, Zhang B, Liu YQ, Wang ZY, Wu YP, Yu XJ, Zhang XD, Ming PH, Zhou GB, Huang L (2013) The natural compound magnolol inhibits invasion and exhibits potential in human breast cancer therapy. Sci Rep 3: 3098.

Melillo G, Scoccianti M, Kovesdi I, Safi J Jr, Riccioni T, Capogrossi MC (1997) Gene therapy for collateral vessel development. Cardiovasc Res **35**: 480-489.

Nikol S, Baumgartner I, Van Belle E, Diehm C, Visona A, Capogrossi MC, Ferreira-Maldent N, Gallino A, Wyatt MG, Wijesinghe LD, Fusari M, Stephan D, Emmerich J, Pompilio G, Vermassen F, Pham E, Grek V, Coleman M, Meyer F. (2008) Therapeutic angiogenesis with intramuscular NV1FGF improves amputation-free survival in patients with critical limb ischemia. Mol Ther **16**: 972–978.

Norgren L, Hiatt WR, Dormandy JA, Nehler MR, Harris KA, Fowkes FG, Rutherford RB (2007) Inter-society consensus for the management of peripheral arterial disease. TASC II Working Group. Int Angiol. 26: 81-157.

Osswald W, Guimarães S (1983) Adrenergic mechanisms in blood vessels: morphological and pharmacological aspects. Rev Physiol Biochem Pharmacol 96: 53-122.

Pugh CW, Ratcliffe PJ (2003) Regulation of angiogenesis by hypoxia: role of the HIF system. Nat Med **9**: 677-684.

Queen LR, Ji Y, Xu B, Young L, Yao K, Wyatt AW, Rowlands DJ, Siow RC, Mann GE, Ferro A (2006) Mechanisms underlying beta2-adrenoceptor-mediated nitric oxide generation by human umbilical vein endothelial cells. J Physiol **576**: 585-594.

Rafii S, Lyden D (2003) Therapeutic stem and progenitor cell transplantation for organ vascularization and regeneration. Nat Med **9**: 702-712.

Rajagopalan S, Mohler ER III., Lederman RJ, Mendelsohn FO, Saucedo JF, Goldman CK, Blebea J, Macko J, Kessler PD,Rasmussen HS, Annex BH (2003) Regional angiogenesis with vascular endothelial growth factor in peripheral arterial disease: a phase II randomized, double-blind, controlled study of adenoviral delivery of vascular endothelial growth factor 121 in patients with disabling intermittent claudication. Circulation **108**: 1933–1938.

Rengo G, Lymperopoulos A, Koch WJ (2009a) Future g protein-coupled receptor targets for treatment of heart failure. Curr Treat Options Cardiovasc Med **11**: 328-338.

Rengo G, Lymperopoulos A, Zincarelli C, Donniacuo M, Soltys S, Rabinowitz JE, Koch WJ (2009b) Myocardial adeno-associated virus serotype 6-βARKct gene therapy improves cardiac function and normalizes the neurohormonal axis in chronic heart failure. Circulation **119**: 89-98.

Rengo G, Leosco D, Zincarelli C, Marchese M, Corbi G, Liccardo D, Filippelli A, Ferrara N, Lisanti MP, Koch WJ, Lymperopoulos A (2010) Adrenal GRK2 lowering is an underlying mechanism for the beneficial sympathetic effects of exercise training in heart failure. Am J Physiol Heart Circ Physiol. **298**: H2032-2038

Rengo G, Lymperopoulos A, Leosco D, Koch WJ (2011) GRK2 as a novel gene therapy target in heart failure. J Mol Cell Cardiol **50**: 785-792.

Rengo G, Zincarelli C, Femminella GD, Liccardo D, Pagano G, de Lucia C, Altobelli GG, Cimini V, Ruggiero D, Perrone-Filardi P, Gao E, Ferrara N, Lymperopoulos A, Koch WJ, Leosco D (2012) Myocardial β(2)-adrenoceptor gene delivery promotes coordinated cardiac adaptive remodelling and angiogenesis in heart failure. Br J Pharmacol **166**: 2348-2361

Rengo G, Cannavo A, Liccardo D, Zincarelli C, de Lucia C, Pagano G, Komici K, Parisi V, Scala O, Agresta A, Rapacciuolo A, Perrone Filardi P, Ferrara N, Koch WJ, Trimarco B, Femminella GD, Leosco D. (2013) Vascular endothelial growth factor blockade prevents the beneficial effects of β-blocker therapy on cardiac function, angiogenesis, and remodeling in heart failure. Circ Heart Fail **6**: 1259-1267.

Salazar NC, Vallejos X, Siryk A, Rengo G, Cannavo A, Liccardo D, De Lucia C, Gao E, Leosco D, Koch WJ, Lymperopoulos A (2013) GRK2 blockade with βARKct is essential for cardiac β2-adrenergic receptor signaling towards increased contractility. Cell Commun Signal **11**: 64.

Sorriento D, Santulli G, Del Giudice C, Anastasio A, Trimarco B, Iaccarino G (2012) Endothelial cells are able to synthesize and release catecholamines both in vitro and in vivo. Hypertension **60**:129-136.

White DC, Hata JA, Shah AS, Glower DD, Lefkowitz RJ, Koch WJ (2000) Preservation of myocardial beta-adrenergic receptor signaling delays the development of heart failure after myocardial infarction. Proc Natl Acad Sci U S A **97**: 5428-5433.

Footnotes

Financial Support: The current study was in part supported by the Italian Ministry of University and Scientific Research-Year 2009 [prot. 2009L4X28T].

The authors A. C. and D. Li. contributed equally.

Figure Legends

Figure 1

βAR downregulation is associated with increased GRK2 protein levels in the ischemic muscle.

A) Bar graph showing blood perfusion in the ischemic hindlimb in rats at 15 days post-femoral artery resection (HI; n=6) and in sham-operated rats (Sham; n=6), as assessed by dyed beads dilution method. Data are expressed as percentage of ischemic to non-ischemic hindlimb; **B)** Bar graphs showing total βAR density on skeletal muscle plasma membrane preparations from rats 15 days post-femoral artery resection (HI; n=6) and sham-operated rats (Sham; n=6); **C)** Representative immunoblots (upper panel) and densitometric analysis (lower panel) of multiple (n=3, including 2 samples per group each) independent experiments showing GRK2/GAPDH protein levels in skeletal muscle lysates from the ischemic hindlimb of rats undergoing femoral artery resection (HI, n=6) and from sham-operated rats (Sham, n=6). GAPDH was used as loading control; Data are expressed as mean ± SEM. *$p<0.05$ vs Sham

Figure 2

In Vivo gene delivery study design

A) Overall study design. Rats underwent femoral resection and were randomized to receive intravascular injection of Ad-βARKct or Ad-GFP or a saline (vehicle). Hindlimb perfusion was evaluated by US-Doppler before, immediately after, 3, 7 10 and 15 days post-surgery. **B)** Rrepresentative immunohistochemistry images showing βARKct/endogenous GRK2 expression in skeletal muscle of rats treated with Ad-βARKct or saline. βARKct was detected using an anti-GRK2 antibody; Scale bar: 100 μm **C-D)** Representative immunoblot **(C)** and densitometric analysis **(D)** of multiple independent experiment (n=4) to evaluate GRK2 and βARKct expression in skeletal muscle lysates of rats treated with Ad-βARKct or saline. GRK2 expression has been normalized with GAPDH, while βARKct expression has been expressed as fold of endogenous GRK2 level.

Figure 3

βARKct gene delivery in skeletal muscle improves post-ischemic angiogenesis and restores β_2AR density.

A) Blood flow measured by US doppler in the tibial posterior artery of rats (n=6-8 rats for each group) over the course of 15 days post-surgery. Data are expressed as percent of ischemic to non-ischemic limb. **B)** Blood perfusion (n=6-8 rats for each group) in the ischemic HL of all 4 study groups as evaluated by dyed beads dilution assay performed at the end of the study period (15 day after gene transfer). Perfusion data are expressed as ischemic-to-non ischemic ratio percent of dyed beads content per milligram of hind-limb muscle tissue. **C)** Representative images of Lectin Bandeiraea simplicifolia I (BS-I) staining of capillaries in the ischemic hindlimb (Left panels; Scale bar: 100 μm) and bar graph (right panel) showing Capillary-to-myocyte ratio in ischemic muscles (n=8 each group) of all 4 groups and in sham-operated rats, as control. Arrows indicate capillaries; **D)** βAR plasma membrane density in skeletal muscle homogenates, purified from hindlimb (n=6 rats for each group) from Sham and ischemic groups (Saline, GFP and βARKct) at 15 days after surgery and gene delivery.

*p<0.05 vs Sham; # p< 0.05 vs Saline and GFP.

Figure 4

Fenoterol selectively stimulates endothelial β_2AR pro-angiogenic signaling in BAECs.

A-B) Representative immunoblots (upper panels) and densitometric quantitative analysis (lower panel) of multiple (n=3) independent experiments to evaluate in bovine aortic endothelial cells (BAECs) unstimulated (Ns) or stimulated with fenoterol (Fen, 1 μM) for 15 minutes: (**A**) Akt phosphorylation levels on serine 473 (^{ser473}p-Akt) and **(B)** eNOS phosphorylation levels on serine 1177 (^{ser1177}p-eNOS) and total protein levels. Total Akt and total e-NOS served as loading controls, respectively. Prior to Fen

stimulation a group of cells was pre-treated with selective β2AR antagonist ICI-118,551 (ICI, 10 μM). *p<0.05 vs Ns.

Figure 5

Effects of GRK2 levels on β_2AR phosphorylation and Akt and eNOS activation following Fen stimulation in BAECs.

A-B-C-D) Representative immunoblots (upper) and densitometric analysis (bottom) of multiple independent experiments (n=3) to evaluate: **(A)** β_2AR phosphorylation levels on threonine 384 (^{thr384}p-β_2AR), **(B)** ^{ser473}p-Akt and **(C)** ^{ser1177}p-eNOS and total protein levels of **(D)** GRK2 in total lysates of BAECs, infected with adenoviruses (Ad) encoding for GFP, GRK2 or βARKct. Cells were Ns of stimulated with Fen (1 μM) respectively for 5 minutes **(A)** or 15 minutes **(B-C-D)**. Total β_2AR, total Akt, total eNOS and GAPDH served as loading controls. Data are expressed as mean ± SEM. *p<0.05 vs GFP Ns; # p< 0.05 vs GFP Fen.

Figure 6

Long-term effects of Fen stimulation on β_2AR function in BAECs.

A-B-C-D) Densitometric analysis of multiple independent experiments to evaluate **(A)** GRK2 protein levels and ^{thr384}p-β_2AR **(B)** ^{ser473}p-Akt **(C)** ^{ser1177}p-eNOS **(D)** in total lysates of BAECs, infected with adenoviruses (Ad) encoding for GFP, GRK2 or βARKct. Cells were Ns of stimulated with Fen (1 μM) respectively for 6 hours (A-B-C-D). GAPDH, total β_2AR, total Akt and total eNOS served as loading controls, respectively; *p<0.05 vs GFP Ns; #p<0.05 vs GRK2.

Figure 7

βARKct prevents fenoterol-induced β_2AR-internalization in BAECs.

A-B) Representative immunoblots **(A)** and densitometric quantitative analysis **(B)** of multiple (n=3) independent experiments to evaluate β_2AR levels in crude plasma membrane preparations and in cytosolic fraction obtained from BAECs infected with Ad-GFP and Ad-βARKct. Cells were not stimulated (Ns) or stimulated with Fen (1 μM) for 6 hours. *p<0.05 vs GFP Ns; #p<0.05 vs GFP Fen; **C)** Representative immunofluorescence images (Scale bar: 10 μm) of β_2AR in BAECs infected with Ad-GFP and Ad-βARKct. Cells were Ns or treated for 6 hours with Fen (1 μM). Arrows indicate receptors that are internalized.

Figure 8

The presence of βARKct enhances BAEC function.

A) Bar graph showing Nitric Oxide (NO) release in the media obtained from BAECs infected with Ad-GFP and –βARKct, Ns or stimulated with Fen (1 μM) for 6 hours. *p<0.05 vs GFP Ns; # p< 0.05 vs GFP Fen. **B)** Representative images (upper; Scale bar: 25 μm) and bar graphs (lower) showing percentage of cell migration in response to 6 hours of Fen (1 μM) stimulation, evaluated by wound healing scratch assay. Confluent monolayers of BAECs infected with Ad-GFP and –βARKct were wounded at time 0 (T = 0). The average rate of wound closure during the first 6 hours of wound healing was calculated from n=3 independent experiments; *p<0.05 vs GFP Ns; # p< 0.05 vs GFP Fen. **C)** BrdU proliferation assay in BAECs, infected with Ad-GFP and –βARKct, at different time points (0, 6 and 24 hours) of stimulation with Fen (1 μM). Results are expressed as percentage of proliferation over Ns cells; *p<0.05 vs GFP Ns; # p< 0.05 vs GFP Fen.

Figure 9

The lack of eNOS prevents the effects of βARKct in ECs

Murine aortic endothelial cells (ECs), isolated from Wild-type (WT) and eNOS KO mice, infected with Ad-GFP or -βARKct, Ns or stimulated with Fen (1 μM). **A)** Bar graphs (lower) showing percentage of cell migration, evaluated by wound healing scratch assay. Confluent monolayers of ECs were wounded at time 0 (T = 0). The average rate of wound closure during the first 6 hours of wound healing was calculated from n=3 independent experiments; **B)** BrdU proliferation assay in ECs at different time points (0, 6 and 24 hours). Results are expressed as percentage of proliferation over Ns cells; *p<0.05 vs GFP Ns; # p< 0.05 vs GFP Fen; ^p<0.05 vs WT GFP; **C)** Bar graph showing Nitric Oxide (NO) release in the media from ECs stimulated with Fen (1 μM) for 6 hours. *p<0.05 vs WT GFP; # p< 0.05 vs WT βARKct.

Figure 1

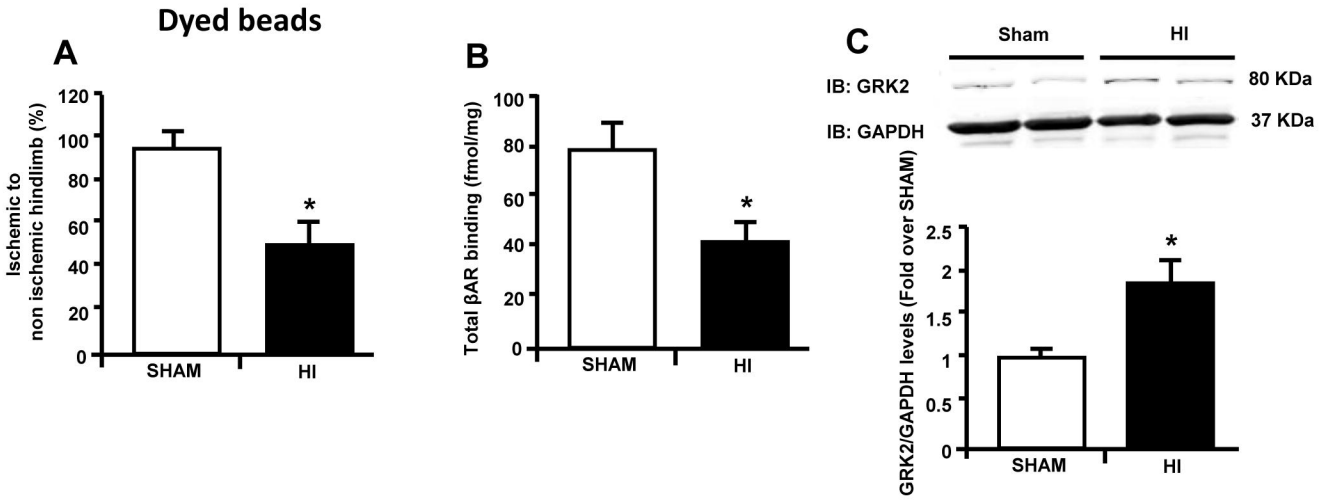
Dyed beads
A
Ischemic to non ischemic hindlimb (%)
120
100
80
60
40
20
0
SHAM
HI
*
B
Total βAR binding (fmol/mg)
100
80
60
40
20
0
SHAM
HI
*
C
Sham
HI
IB: GRK2
80 KDa
IB: GAPDH
37 KDa
GRK2/GAPDH levels (Fold over SHAM)
2.5
2
1.5
1
0.5
0
SHAM
HI
*

Figure 2

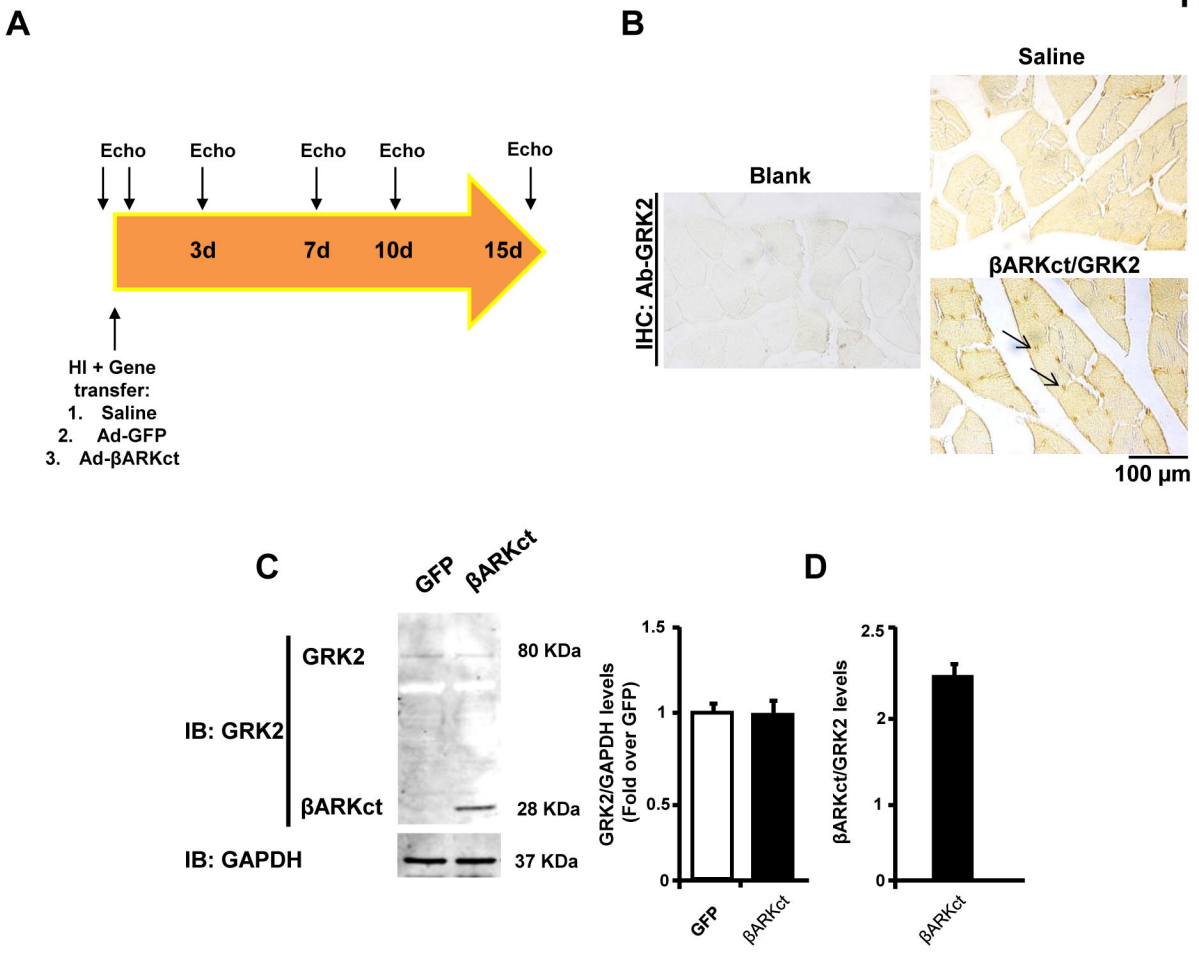
A
Echo
Echo
Echo
Echo
Echo
3d
7d
10d
15d
HI + Gene transfer:
1. Saline
2. Ad-GFP
3. Ad-βARKct
B
Saline
Blank
IHC: Ab-GRK2
βARKct/GRK2
100 μm
C
GFP
βARKct
GRK2
IB: GRK2
βARKct
80 KDa
28 KDa
IB: GAPDH
37 KDa
D
GRK2/GAPDH levels (Fold over GFP)
1.5
1
0.5
0
GFP
βARKct
βARKct/GRK2 levels
2.5
2
1
0
βARKct

Figure 3

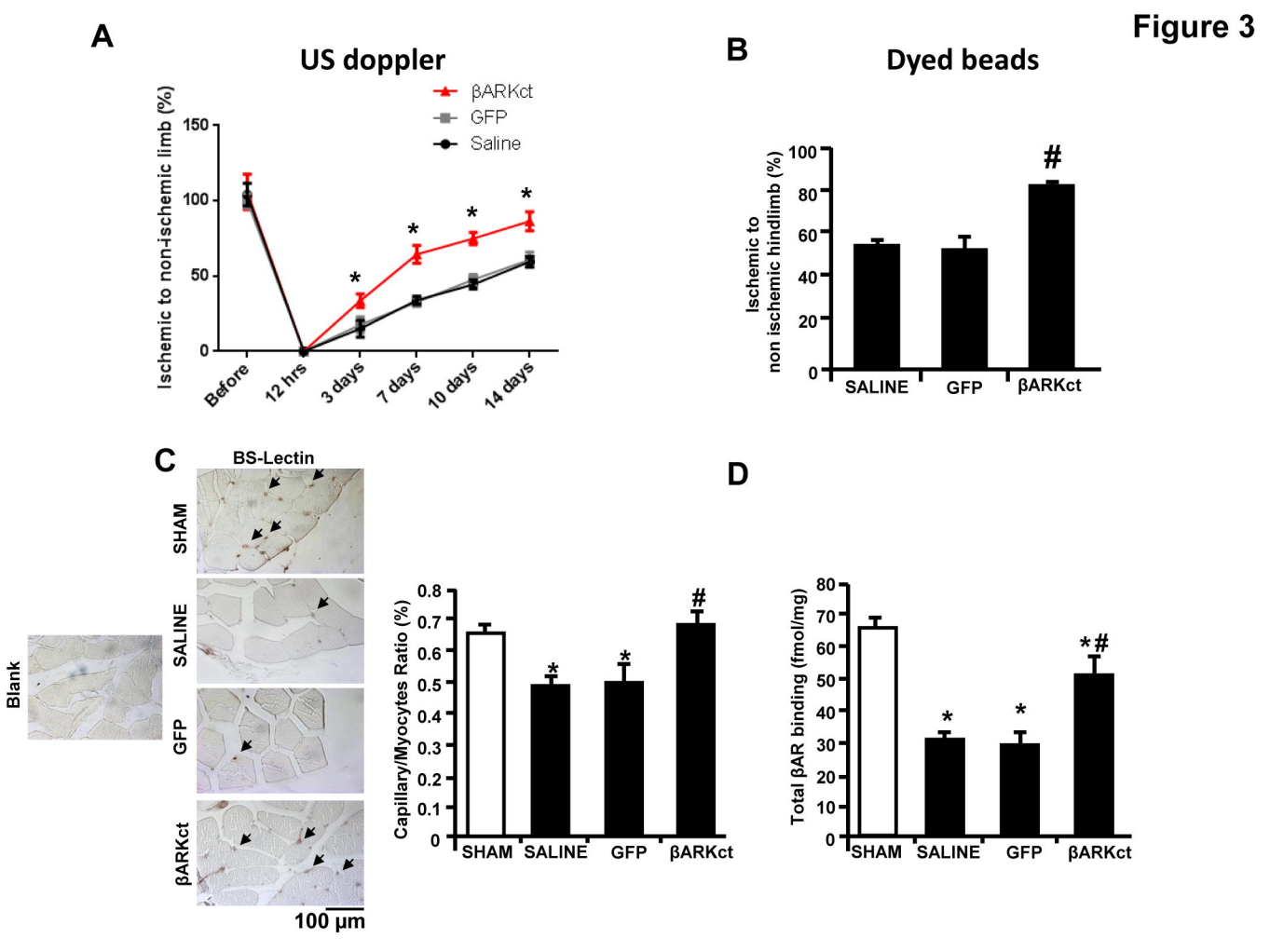
A
US doppler
βARKct
GFP
Saline
Ischemic to non-ischemic limb (%)
150
100
50
0
Before
12 hrs
3 days
7 days
10 days
14 days
*
B
Dyed beads
Ischemic to non ischemic hindlimb (%)
100
80
60
40
20
0
#
SALINE
GFP
βARKct
C
BS-Lectin
SHAM
SALINE
GFP
βARKct
Blank
100 μm
Capillary/Myocytes Ratio (%)
0.8
0.7
0.6
0.5
0.4
0.3
0.2
0.1
0
SHAM
SALINE
GFP
βARKct
D
Total βAR binding (fmol/mg)
80
70
60
50
40
30
20
10
0
*#

Figure 4

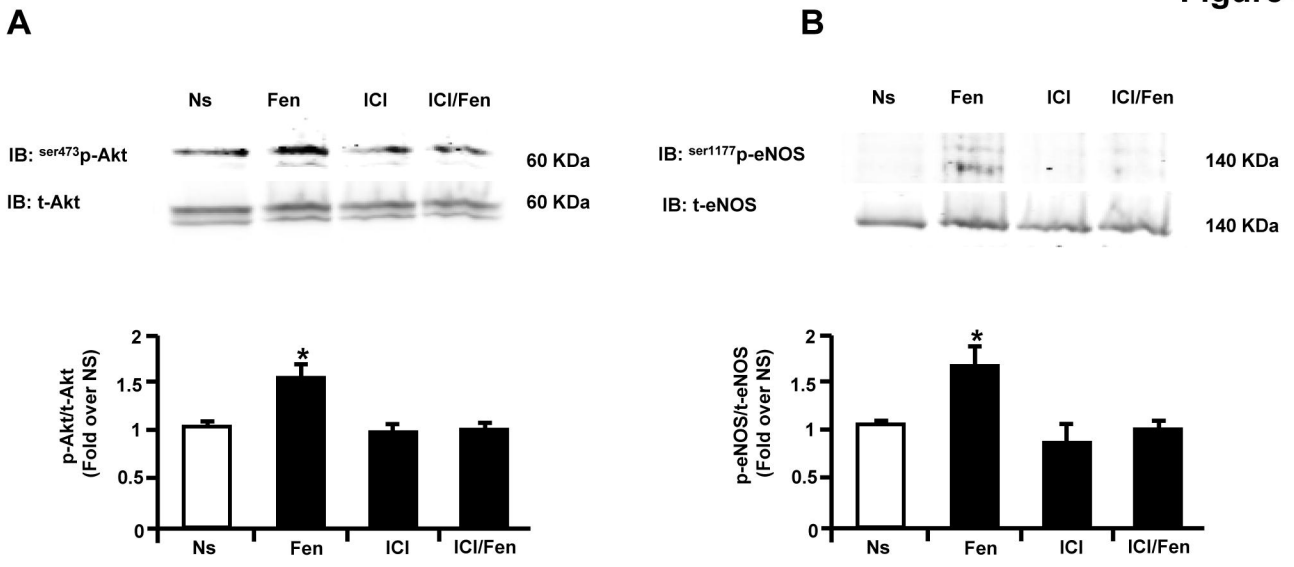
A
Ns
Fen
ICI
ICI/Fen
IB: ser473p-Akt
60 KDa
IB: t-Akt
60 KDa
p-Akt/t-Akt
(Fold over NS)
2
1.5
1
0.5
0
*
Ns
Fen
ICI
ICI/Fen
B
Ns
Fen
ICI
ICI/Fen
IB: ser1177p-eNOS
140 KDa
IB: t-eNOS
140 KDa
p-eNOS/t-eNOS
(Fold over NS)
2
1.5
1
0.5
0
*
Ns
Fen
ICI
ICI/Fen

Figure 5

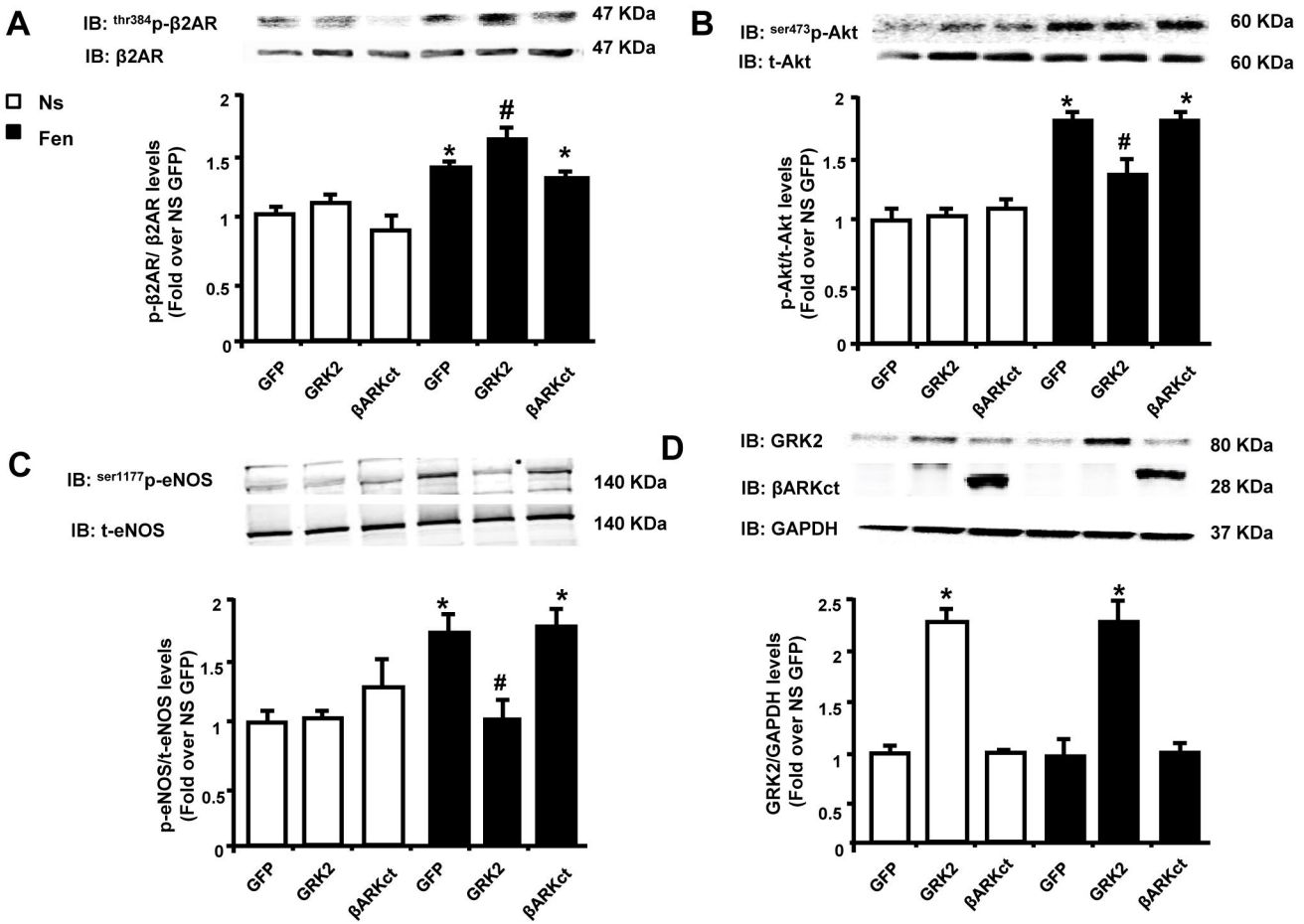
A
IB: thr384p-β2AR
IB: β2AR
47 KDa
47 KDa
Ns
Fen
p-β2AR/ β2AR levels
(Fold over NS GFP)
GFP
GRK2
βARKct
GFP
GRK2
βARKct
B
IB: ser473p-Akt
IB: t-Akt
60 KDa
60 KDa
p-Akt/t-Akt levels
(Fold over NS GFP)
C
IB: ser1177p-eNOS
IB: t-eNOS
140 KDa
140 KDa
p-eNOS/t-eNOS levels
(Fold over NS GFP)
D
IB: GRK2
IB: βARKct
IB: GAPDH
80 KDa
28 KDa
37 KDa
GRK2/GAPDH levels
(Fold over NS GFP)

Figure 6

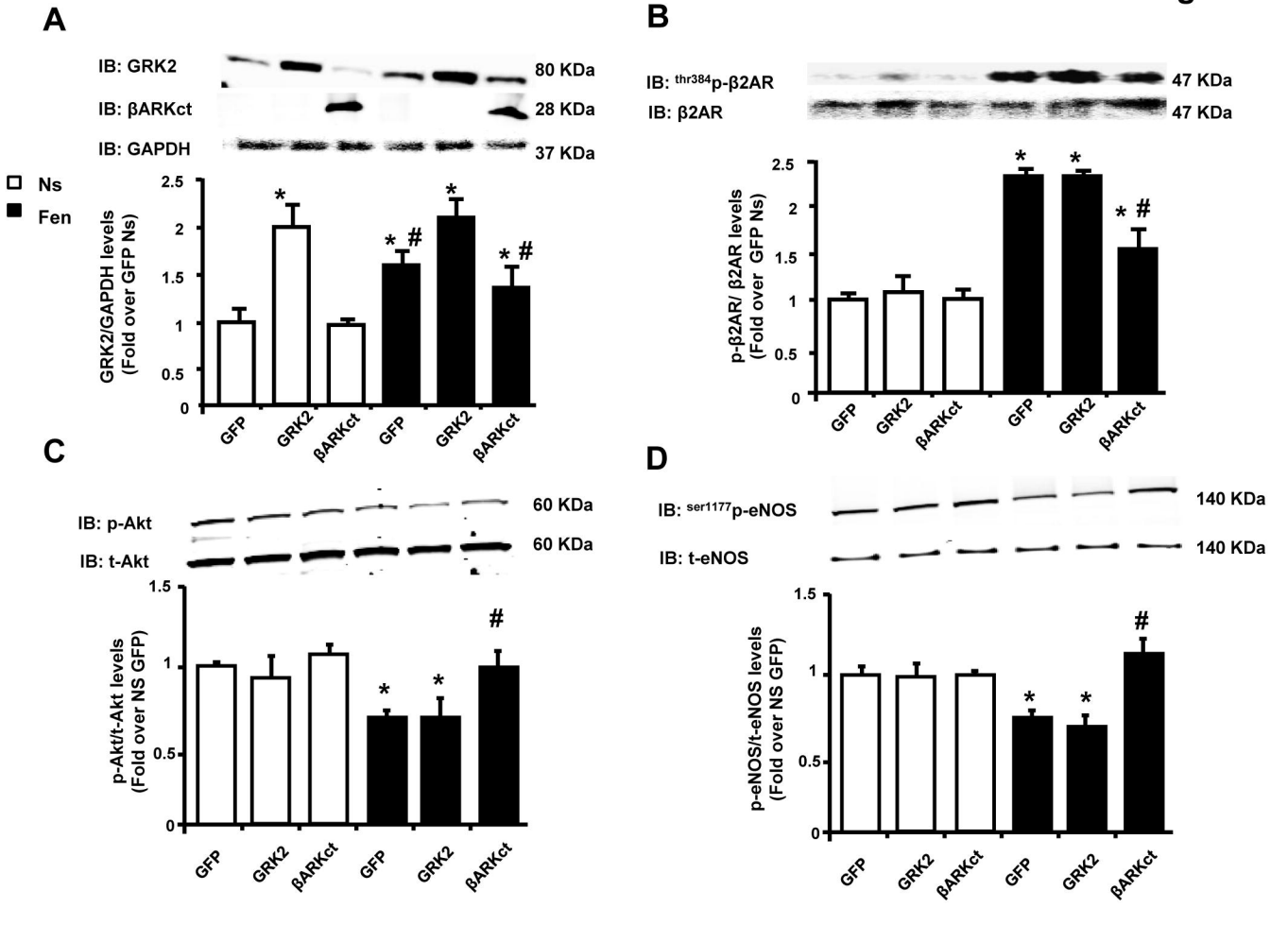
A
IB: GRK2
80 KDa
IB: βARKct
28 KDa
IB: GAPDH
37 KDa
Ns
Fen
GRK2/GAPDH levels (Fold over GFP Ns)
GFP
GRK2
βARKct
B
IB: thr384p-β2AR
47 KDa
IB: β2AR
47 KDa
p-β2AR/ β2AR levels (Fold over GFP Ns)
C
IB: p-Akt
60 KDa
IB: t-Akt
60 KDa
p-Akt/t-Akt levels (Fold over NS GFP)
D
IB: ser1177p-eNOS
140 KDa
IB: t-eNOS
140 KDa
p-eNOS/t-eNOS levels (Fold over NS GFP)

Figure 7

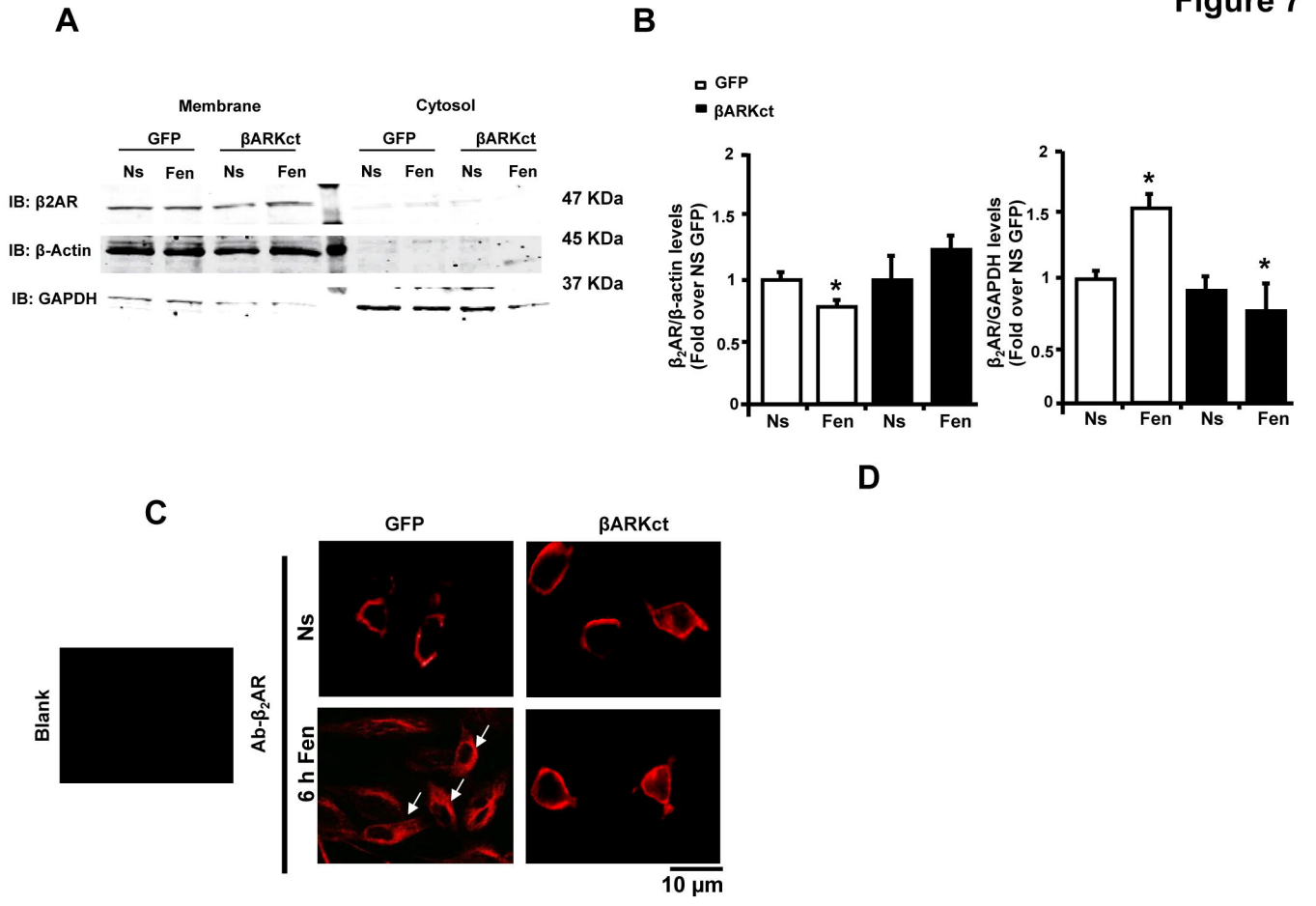
A
Membrane
Cytosol
GFP
βARKct
GFP
βARKct
Ns
Fen
Ns
Fen
Ns
Fen
Ns
Fen
IB: β2AR
IB: β-Actin
IB: GAPDH
47 KDa
45 KDa
37 KDa
B
GFP
βARKct
β2AR/β-actin levels (Fold over NS GFP)
β2AR/GAPDH levels (Fold over NS GFP)
2
1.5
1
0.5
0
*
Ns
Fen
Ns
Fen
C
GFP
βARKct
Blank
Ab-β2AR
Ns
6 h Fen
10 μm
D

Figure 8

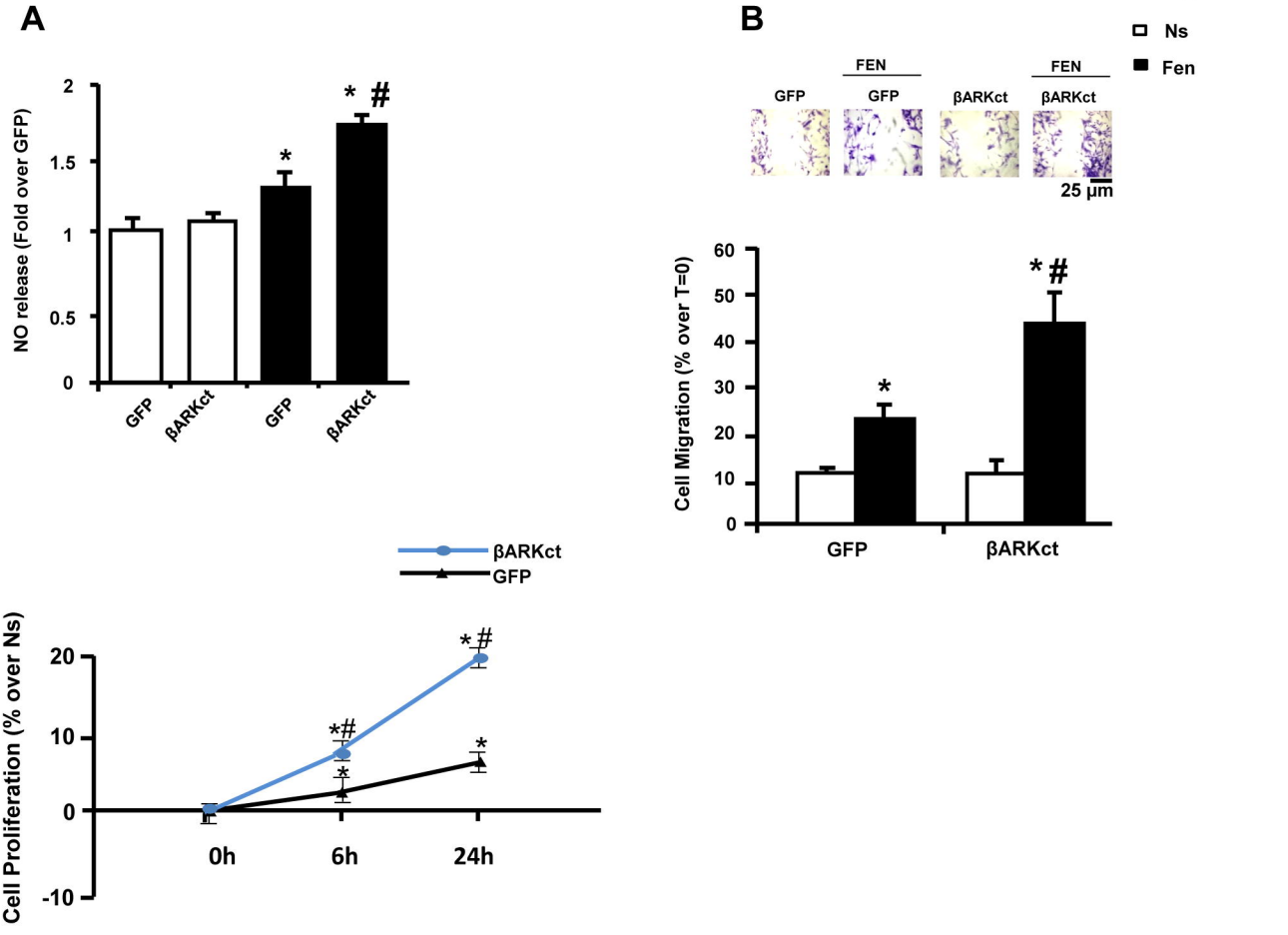
A
NO release (Fold over GFP)
2
1.5
1
0.5
0
*
* #
GFP
βARKct
GFP
βARKct
B
Ns
Fen
FEN
FEN
GFP
GFP
βARKct
βARKct
25 µm
Cell Migration (% over T=0)
60
50
40
30
20
10
0
*
* #
GFP
βARKct
βARKct
GFP
Cell Proliferation (% over Ns)
20
10
0
-10
*#
*
*#
*
0h
6h
24h

Figure 9

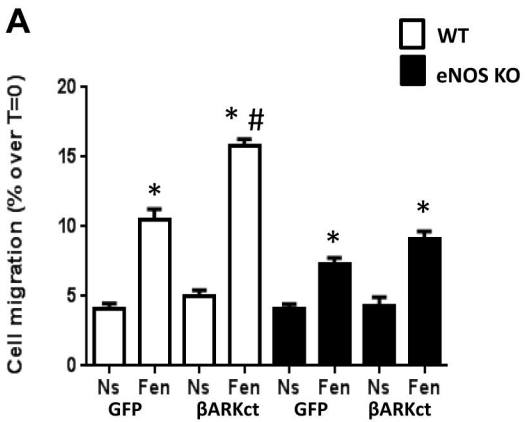
A
WT
eNOS KO
Cell migration (% over T=0)
20
15
10
5
0
* #
*
*
*
Ns Fen Ns Fen Ns Fen Ns Fen
GFP βARKct GFP βARKct

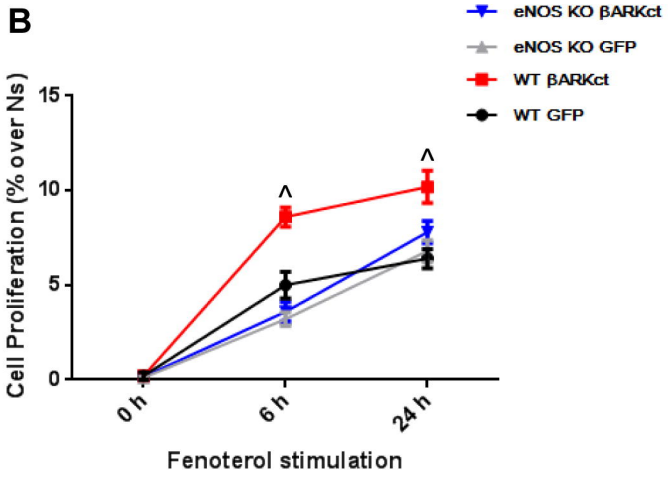
B
eNOS KO βARKct
eNOS KO GFP
WT βARKct
WT GFP
Cell Proliferation (% over Ns)
15
10
5
0
^
^
0 h
6 h
24 h
Fenoterol stimulation

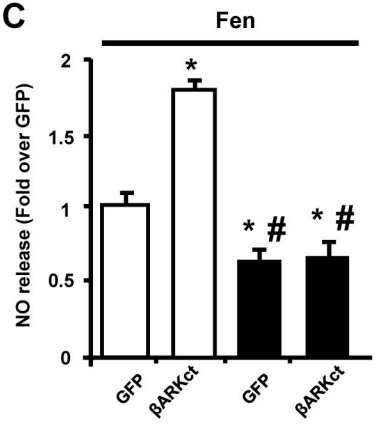
C
Fen
NO release (Fold over GFP)
2
1.5
1
0.5
0
*
* #
* #
GFP
βARKct
GFP
βARKct